Macroscopic Carbon Nanotube Assemblies: Preparation, Properties, and Potential Applications

*Luqi Liu, Wenjun Ma, and Zhong Zhang**

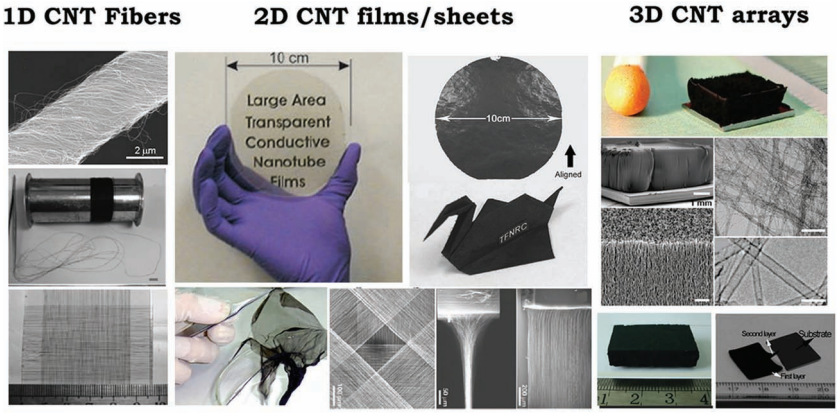

From the Contents

1. Introduction 1505
2. Preparation of Macroscopic CNT Assemblies 1505
3. Mechanical Properties of CNT Assemblies 1511
4. Applications of CNT Assemblies 1515
5. Conclusion and Outlook 1517

As classical 1D nanoscale structures, carbon nanotubes (CNTs) possess remarkable mechanical, electrical, thermal, and optical properties. In the past several years, considerable attention has been paid to the use of CNTs as building blocks for novel high-performance materials. In this way, the production of macroscopic architectures based on assembled CNTs with controlled orientation and configurations is an important step towards their application. So far, various forms of macroscale CNT assemblies have been produced, such as 1D CNT fibers, 2D CNT films/sheets, and 3D aligned CNT arrays or foams. These macroarchitectures, depending on the manner in which they are assembled, display a variety of fascinating features that cannot be achieved using conventional materials. This review provides an overview of various macroscopic CNT assemblies, with a focus on their preparation and mechanical properties as well as their potential applications in practical fields.

NANO MICRO small

1. Introduction

Owing to their remarkable electrical, mechanical, thermal, and optical properties, carbon nanotubes (CNTs) have shown great potential for use in a variety of applications, such as electrodes, actuators, filters, ultrafast photonics, structural fibers, and so forth.[1–3] Meanwhile, the most promising potential employment of CNTs (especially, single-walled carbon nanotubes, SWNTs) is as a novel type of electronic material, due to their outstanding ballistic electronic conduction and insensitivity to electromigration.[4–7] CNTs are able to withstand current densities up to 10^9 A cm^{-2}, which is a thousand times greater than that of noble metals.[8,9] Moreover, a high charge mobility (up to ≈10 000 cm^2 V^{-1} s^{-1}) together with its ballistic transport characteristics render CNTs especially promising as the active channels of transistors in stretchable logic circuits.[10,11] Many theoretical and experimental works have revealed CNTs to be stiff, strong, and highly flexible nanoscale fibers, with a tensile modulus and individual nanotube strength of up to 1 TPa and 63 GPa, respectively, which surpasses all existing materials.[12,13] The density-normalized strength of an individual CNT is around 50 times larger than that of a steel wire.[14] In addition, the thermal conductivity of an individual nanotube can reach 3500 W m^{-1} K^{-1}, showing promising for their use as tiny cooling elements on silicon chips.[15–17]

In order to fully utilize the excellent mechanical and physical properties of individual CNTs at a macroscopic level, it is desirable to fabricate various macroscopic CNT-based materials. Over the past decade, considerable attention has been directed toward the post-processing of nanotube suspensions and/or nanotube–polymer blends.[18] Well-dispersed CNT-based polymer composites have shown remarkable mechanical and electrical properties as compared to conventional microfiller-incorporated composites.[19–22] Laboratory work has produced composite fibers with an excellent tensile strength (4.2 GPa) and tensile modulus (176 GPa) by incorporating SWNTs in a high-strength, high-modulus polymer.[23] Despite many notable achievements with nanotubes in the envisioned application areas, such as super-tough CNT-based poly(vinyl-alcohol) composite fibers (570 J g^{-1}),[24] there are many daunting challenges to be met before maximizing the utilization of the superb mechanical and physical properties of individual nanotubes at the macroscopic level. The most important three of these are the ability to synthesize CNTs with well-controlled morphologies (including diameter, chirality, length, and type), the development of reliable methods that yield good reproducibility of the achieved properties, and improvements to the material properties, which are currently far below theoretical predictions. The first two challenges arise from the absence of techniques and methods that would allow sufficient control to maintain the properties of nanotubes during the synthesis and subsequent post-treatments (e.g., chemical modification of CNTs, and separation of SWNTs). The last challenge lies in the ambiguity of the key factors affecting the nanotubes' behavior, especially for nanotube-blended composites. Alternatively, the direct production of macroscopic CNT assemblies with controlled orientation and configurations by using individual nanotubes as building blocks, becomes an important step towards their potential application. Thus far, significant efforts have been made to fabricate various macroscale CNT assemblies, e.g., CNT fibers, CNT films, and CNT arrays, which provide a great opportunity to realize CNT properties at the macroscale level. Aside from the maintenance of unique properties of individual nanotubes at macroscopic scales, another advantage of CNT assemblies is that they are easily handled and utilized under various conditions. Moreover, the macroscopic CNT assemblies are endowed with novel properties beyond those predicted by theory. For example, 2D conductive CNT films display excellent mechanical flexibility, stretchability, and optical transparence. Such CNT films could not only act as conductive electrodes, but could also be developed into practical magnet-free loudspeakers or artificial muscles.[25,26] The 3D aligned CNT arrays with properly engineered surfaces could work as dry adhesive tapes to biomimic gecko feet.[27,28] The light weight, high porosity, and large surface areas of 3D CNT-based architectures make them promising candidates for environmental applications such as sorption, separation and filtration.[29–33] Low-density 3D CNT arrays could also be engineered to have an extremely low index of refraction, potentially acting as the darkest ever man-made material.[34]

This article reviews the state-of-the-art progress in this relatively new field, with an emphasis on the advanced preparation techniques and mechanical performances of macroscopic CNT assemblies. The first section focuses on the preparation methodologies used up to now. After a summary of the remarkable mechanical properties of various CNT assemblies, their potential applications are envisioned. The last section concludes with some perspectives on the challenges and opportunities of future work.

2. Preparation of Macroscopic CNT Assemblies

Assembly of individual CNTs into macroscopic ordered structures with properties reflecting a significant proportion of those seen in the individual nanotubes remains a challenge to materials processing. The synthesized macroscopic CNT architectures will be described according to their geometry as well as their fabrication methods, namely,

Dr. L. Liu, Prof. Z. Zhang
National Center for Nanoscience and Technology
China, Beijing 100190, P.R. China
E-mail: zhong.zhang@nanoctr.cn
Dr. W. Ma
Max Planck Institute of Quantum Optics
Hans-Kopfermann-Strasse 1, D-85748 Garching, Germany
Prof. Z. Zhang
Center for Nano and Micro Mechanics
Tsinghua University
Beijing 100084, P.R. China

DOI: 10.1002/smll.201002198

1D CNT fibers, 2D CNT films or sheets, and 3D CNT assemblies.

2.1. 1D CNT Fibers

As-synthesized CNT powders are generally tens of micrometers in length and highly entangled. This feature of random orientation of nanotubes at a macroscopic level greatly hampers their use in potential applications, particularly in the composite fields. To fully utilize the excellent axial properties of CNTs, it is justifiable to make CNT-based fiber materials in which nanotube fillers are well aligned along the fiber axis. Melt-spinning of CNT-based polymer composites is a versatile method to orient nanotubes along the fiber axis.[35] In most cases, however, the resulting fibers suffer from poor mechanical and electrical performances owing to the limitations of the high weight content of the incorporated nanotubes as well as to the presence of the polymer matrices. Therefore, the fabrication of macroscopic 1D, neat CNT fibers without trading-off the multiple functionalities of nanotubes has become one of the central goals of material scientists. During the past several years, there have been numerous reports in the literature of the fabrication of neat CNT fibers through a wide range of technologies. Even though, in most cases, the mechanical performance of the fabricated CNT fibers is not still comparable to that of commercial fibers (e.g., carbon fiber, Kevlar), their flexibility, high conductivity and other characteristics have shown great promise in a variety of applications such as structural materials,[36] strong and highly conductive cables,[37] electrochemical actuators,[38] incandescent bulb filaments,[39] and so forth.[40]

2.1.1. Direct Synthesis of 1D CNT Fibers

To sustain the superior mechanical and electrical properties of individual nanotubes in the macroscopic CNT fibers, it is required that individual nanotubes are grown as long as possible and intertube binding forces are made as strong as possible. However, it is a difficult task to directly synthesize individual CNTs of up to centimeter scales in a furnace.[41,42] Alternatively, the assembly of individual nanotubes via Van der Waals interactions may be an effective approach to fabricate 1D CNT fibers. Over the past ten years, great efforts have been devoted to fabricate long CNT fibers. An encouraging breakthrough was made by Zhu et al, where macroscopic SWNT strands were fabricated with tens to hundreds of micrometers thickness and several centimeters long (**Figure 1**a) through a vertically floating chemical vapor deposition (CVD) method.[43] Even though this work showed the possibility of directly forming CNT strands in a furnace, the products still suffered from severe limitations in terms of length, the isolated morphology of yielded strands, production efficiency, and stability.

2.1.2. Spinning 1D CNT Fibers from CNT Aerogel

Adopting a similar method to that reported by Zhu et al.[43] in 2004, Li et al. made continuous CNT fibers by mechanically drawing CNT aerogel from the gaseous reaction zone, and then directly winding it onto a rotating rod as shown in Figure 1b.[44] The key requirements for continuous spinning are the rapid production of high purity nanotubes to form an aerogel in the furnace hot zone and the forcible removal of the product from reaction chamber by continuous wind-up. The fabrication of CNT fibers greatly relies on the assembly of CNTs in the gas flow via van der Waals interactions. To effectively assemble the CNTs into a continuous integrated 'sock' in the furnace, ethanol or acetone vapor are usually employed as carbon sources.[45] In this case, the best electrical conductivity of as-received CNT fibers was $8.3 \times 10^3\ \Omega^{-1}\ cm^{-1}$, and the tensile strength had a wide range between 0.10 and 1 GPa.[44] The microstructure of spinning CNT fibers is heavily dependent on the synthetic conditions

LuQi Liu is currently an associate professor at the National Center for Nanoscience and Technology, China (NCNST). She received her PhD from the Institute of Chemistry at the Chinese Academy of Sciences in 2003. After that, she undertook postdoctoral research in the Department of Materials and Interfaces at the Weizmann Institute of Science (Israel). In March 2007, she joined NCNST. Her current research focuses on the mechanics of polymer-based nanocomposites.

Wenjun Ma is currently a postdoc working at the Max Planck Institute of Quantum Optics in Germany. He received his PhD from Institute of Physics, Chinese Academy of Sciences in 2009 under the supervision of Prof. Sishen Xie. For his thesis, entitled 'Study on the on Preparation and Physical Properties of Macroscale Single-walled Carbon Nanotube Architectures', he was awarded 'The Outstanding Graduates Award of Chinese Academy of Sciences' and 'The Outstanding PhD Dissertation Award in Beijing'. His current research interest is the design and manufacture of novel targets for ultra-intense lasers and the physics of ultra-intense laser–matter interactions.

Zhong Zhang is currently Professor and Head of the 'Nanomanufacturing and Applications' division at the National Center for Nanoscience and Technology, China. He received his PhD in 1999 and, as an Alexander von Humboldt Sofja Kovalevskaja Award winner, served as a visiting professor and group leader at the Institute for Composite Materials at the University of Kaiserslautern in Germany 2001–2005, before moving back to China in 2006. His major research interests are hierarchically structured polymer nanocomposites, nanostructured surfaces and coatings, nanomanufacturing and applications. He serves as an editorial board member of 6 leading academic journals. He currently also serves as the Vice President of the Chinese Society of Particuology and the Deputy Secretary General of the Chinese Society for Composite Materials.

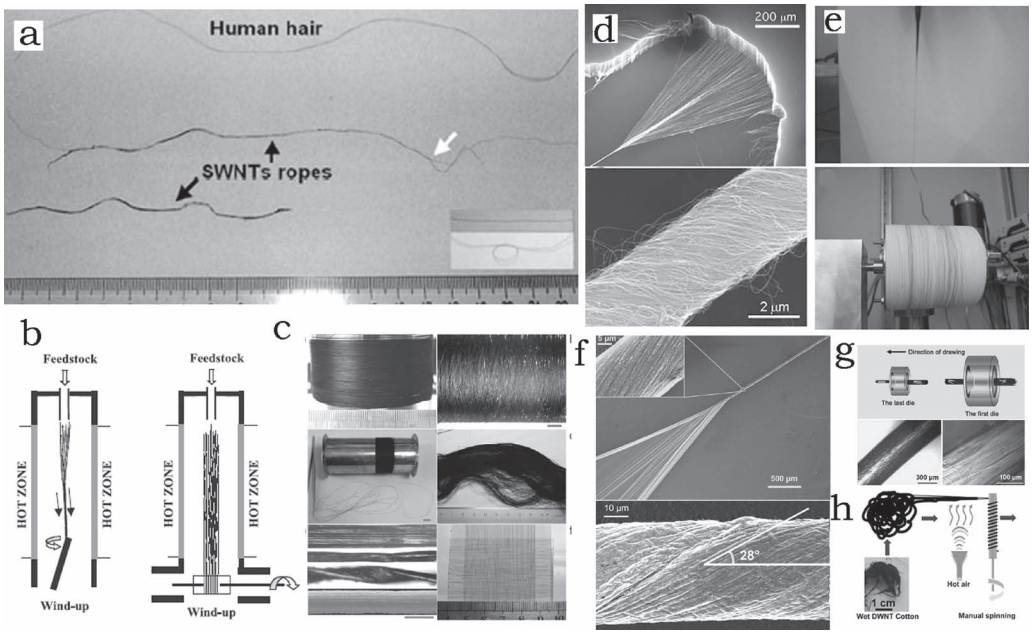

Figure 1. a) Optical image of as-grown SWNT strands by direct synthesis method. Reproduced with permission from Ref.[43]. Copyright 2002, The American Association for the Advancement of Science (AAAS). b) Schematic of spinning CNT fibers and sheets from a CNT aerogel. Reproduced with permission from Ref.[44]. Copyright 2004, AAAS. c) Multilayered CNT yarns and products. Reproduced with permission from Ref.[37]. d) Scanning electron microscope (SEM) images of spinning a CNT fiber from a 3D CNT array and the resulting fiber. Reproduced with permission from Ref.[47]. Copyright 2004, AAAS. e) Wet spinning process to produce CNT fibers. Reproduced with permission from Ref.[54]. Copyright 2004, AAAS. f) SEM images of twisting SWNT fiber from its film and resulting fiber.[59] g) Schematic of drawing SWNT fiber through diamond wire dies and optical images of the resulting fiber. Reproduced with permission from Ref.[60]. Copyright 2008, American Chemical Society (ACS). h) Schematic of drawing–drying spinning process for fabricating DWNT fibers. Reproduced with permission from Ref.[62].

as well as the spinning velocities: the processing parameters to fabricate practically useful CNT fibers with controllable electrical and mechanical properties must be further optimized. On the basis of their prior work,[44,45] recently Li et al. further advanced this approach and employed a mixture of ethanol and acetone vapor as the carbon source to fabricate novel continuous CNT fibers with a multilayered structure.[37] The final length of the continuous fibers reached several kilometers, and the macroscale uniformity of the as-spun fibers was close to conventional textile fibers (Figure 1c). This unique 'tube-in-tube' hollow structure of the as-produced CNT fibers, combined with their high electrical conductivity (5000 S cm^{-1}), might have potential application as a functional fabric in energy-storage fields.

2.1.3. Spinning of 1D CNT Fibers from Super-Aligned CNT Arrays

By mimicking the process of drawing silk out of a cocoon, Jiang et al. were the first to report spinning of the continuous CNT fibers from free-standing, super-aligned CNT array.[46] Afterwards, considerable attention was attracted to this field for improving the properties of CNT fibers using a variety of techniques. In 2004, Zhang et al. introduced a twisting approach to the spinning CNT threads to make single or multi-ply twisted fibers (Figure 1d).[47] Owing to the introduced intertube mechanical coupling by twisting, the intertube slippage and sliding of CNT fibers was effectively prevented, and the electrical conductivity of the nanotubes was maintained. The measured electrical conductivity of CNT fibers was ≈300 S cm^{-1} at room temperature and their tensile strength was in the range of 200–500 MPa. It is noteworthy that both the tensile strength and modulus of as-spun CNT fibers are not still comparable to that of fibers spun from aerogel. Microstructure characterizations have identified that the former CNT fibers possess a joined end-to-end structure among nanotubes,[48] which would greatly affect the mechanical and electrical behavior of the resulting CNT fibers. To further improve the mechanical properties of CNT fibers, post-spin twisting was carried out to prohibit the slippage of nanotubes, as proposed by Zhang et al.[49] The final tensile strength of CNT fibers could then reach up to 2 GPa.

Significant developments on CNT fiber fabrication based on super-aligned CNT arrays have been achieved,[47] whereas the strategy to continuously manufacture CNT fibers on an industrial scale with controllable mechanical properties is still in an early stage. Following on from their serial of works regarding aligned CNT arrays as well as CNT fibers or sheets,[46,48] recently, Jiang and co-workers reported a simple and continuous spinning method to produce CNT fibers, especially to prepare the ultra-thin fibers with a diameter of less than 10 μm.[50] The main advantage of this method is possibly its feasibility in future industry. CNT fibers with a wide range of diameters could be generated easily according to the width of the aligned CNT array using the laser etching method. However, voids or inclusions would inevitably be introduced into fibers during the twisting process, and subsequently compromise the

properties of CNT fibers. Accordingly, fibers freshly spun from a super-aligned CNT array were first twisted and then passed through a volatile solvent (e.g., acetone, ethanol) for shrinking. Thus, the tensile strength of as-produced CNT fibers consisting of highly densely packed nanotubes was up to 1GPa.[50,51]

On the basis of the traditional textile spinning principles, recently, Tran et al. used a modified twisting method by adding a 'tensioning zone' into the twisting system, and obtained CNT fibers with tensile strengths of up to 1 GPa.[52] However, the tensioning zone introduced an extra tension force, which is unfavorable for preparing ultra-thin fibers that are prone to breaking under the tension during the twisting process.

2.1.4. Conventional Wet Spinning of 1D CNT Fibers

Coagulation spinning has been widely used for making various organic fibers, such as Kevlar, acrylic, and poly(acrylonitrile) fibers. In this process, a polymer solution is extruded into a bath that contains a second liquid in which the solvent is soluble but the polymer is not. The polymer therefore phase-separates and condenses to form a fiber. Unlike the solubility of the polymer, the intrinsic chemical inertness as well as the aggregated feature of CNTs limits their solubility in aqueous, organic, or acid media. Although the addition of surfactants could improve CNT solubility, the surfactants adsorbed onto nanotube surfaces has tended to poison the outstanding electrical and thermal properties of the nanotubes. Briefly, it seemed to be unfeasible to directly spin pristine CNTs via the wet spinning technique. Based on their prior work, in which SWNTs could be dissolved in sulfuric acid fumes,[53] an encouraging breakthrough was made by Ericson et al. in 2004, in which the macroscopic, continuous, neat SWNT fibers were successfully spun from a suspension of nanotubes in superacids (Figure 1e).[54] X-ray Diffraction (XRD) characterization further indicated that the alignment of nanotubes within the fibers was ±15.5°. The Young's modulus of the resulting fibers approached 120 GPa, closer to that of Kevlar fibers. Despite the poor toughness of neat CNT fibers compared to SWNT–PVA composites,[24,55] however, the CNT fibers had excellent electrical (5000 S cm^{-1}) and thermal conductivities (21 W km^{-1}) due to the absence of polymer. To further improve the spin-processibility of SWNT solutions, recently, chlorosulphonic acid was utilized to enhance nanotube solubility in the liquid phase.[56] For example, the weight concentration of SWNTs in chlorosulphonic acid could reach up to 0.5 wt%, 1000 times higher than previously reported superacids. The highly concentrated nanotube solutions would also favor the formation of liquid-crystal domains, and thus nanotubes could be readily processed into macroscopic fibers or sheets with controlled morphologies. Mechanical tests have indicated that the typical strength of obtained SWNT fibers ranged from 50 to 150 MPa, with some spinning tests yielding strengths in excess of 320 MPa. The typical modulus was 120 GPa, similar to previous results.[54] Even though such significant progress greatly encouraged the engineering of macroscopic SWNT fibers or films, this method was not effective for the fabrication of MWNT-based fibers. Recently, Zhang et al. reported a simple coagulation process to spin fibers consisting of MWNTs directly from their lyotropic liquid-crystalline phase, in which ethylene glycol was employed as dispersant.[57] The modulus of N-doped MWNT fibers was 142 ± 70 GPa, with a fracture stress 0.17 ± 0.07 GPa. The relatively wide range of the modulus was attributed to the existence of voids and defects during the fiber-spinning process. Further optimization of the spinning process is imperative to improve the mechanical properties of MWNT fibers.

The CNT fibers described above commonly possess monolithic structures with excellent mechanical properties, and thereby have potential application in composite fields. Specifically, the hollow structure of the CNT fibers with high electrical conductivity is required for their use as supercapacitors, batteries, and artificial muscles in liquid media. Based on their previous polymer-based coagulant spinning method,[24] Kozlov et al. further advanced the polymer-free spinning process to fabricate hollow SWNT fibers with electrical conductivities ~140 S cm^{-1} and an electrochemical capacitance ~100 F g^{-1}.[58]

2.1.5. Spinning of 1D Fibers from CNT Films

Similar to the methods employed in industrial fields to fabricate fiber materials, Figure 1f shows a typical twisting process for the manufacture of SWNT fibers using anisotropic SWNT films as starting materials.[59] In comparison with existing spinning methods proposed by other groups, the film-twisting method could more easily control the diameters and twisting degrees of SWNT fibers. By utilizing the same SWNT films as starting materials, Liu et al. developed a low-cost and effective method to fabricate highly dense and aligned SWNT fibers via a series of diamond wire-drawing dies as shown in Figure 1g.[60] XRD characterization demonstrated that the SWNT fibers formed crystalline structure through van der Waals forces when they were perfectly aligned and ideally densely packed. The resistivity of fibers was close to 2 mΩ cm at room temperature. Recent work has demonstrated that such fibers could convert the surface energy of liquids into electricity, and thereby they could serve as a self-powered system to drive a thermistor.[61] Nevertheless, it should be pointed out that the methods described above aren't feasible for the fabrication of continuous SWNT fibers owing to the discontinuity of SWNT films in the current case.

2.1.6. Other Methodologies

By mimicking the ancient cotton-spinning process, Ci et al. developed an efficient draw–drying process to fabricate continuous double-walled carbon nanotube (DWNT) fibers from randomly oriented DWNT 'cotton', as presented in Figure 1h.[62] The mechanically robust as-spun fibers showed the potential for use as efficient electron emission sources as well as electrodes for electrochemical sensing.

2.2. 2D Free-Standing CNT Films

Free-standing CNT films or sheets can generally be fabricated by either suspension-based deposition or CVD growth approaches. The main advantages of as-prepared CNT films are their many potential applications based on their excellent

NANO MICRO small

properties, such as mechanical stability, flexibility, remarkable electrical and thermal conductivities, and chemical stability. For example, the free-standing MWNT sheets exhibit higher density-normalized strength (≈465 MPa (g cm^{-3})$^{-1}$) together with high electrical conductivity (700 Ω □$^{-1}$) and optical transparency.[63] Recently, numerous reports have demonstrated that CNT films show potential for such applications as energy storage devices,[64–68] sensors,[69] electronic devices,[70–72] field-effect transistors,[73] polarized light sources,[46,63] and loudspeakers.[25] In particular, the extraordinary electrical properties of CNT films, together with their optical transparency, has greatly stimulated development in the flexible and stretchable thin-film-based electronics and optoelectronics. Several reviews have summarized the advances of transparent-CNT-film manufacturing through suspension-based deposition approaches, and this will therefore not be discussed in great detail here.[74–76]

2.2.1. Suspension-Based Post-Treatments

Even though various techniques based on CNT suspensions have been developed to fabricate macroscopic 2D CNT films, such as spin coating,[77] drop drying from solvents,[78] Langmuir–Blodgett deposition,[79] and airbrushing.[80] Unfortunately, most of the fabricated CNT films with thicknesses of a few hundred nanometers have to be supported by a substrate. Thus, special transfer techniques are required to release the paperlike film to the desired substrate, which may cause damage to the resulting product. In comparison with the ultrathin CNT films, CNT films with micrometer thicknesses could directly be peeled off the filtration membrane. The first free standing macroscopic SWNT film, the so-called "Bucky paper", was fabricated by means of a SWNT-suspension-based vacuum-filtration method.[81] Herein, SWNTs were first dispersed in solution with the help of a surfactant and ultrasonication, and then the SWNT suspensions were filtered under vacuum to form a film. The film thickness was readily controlled by the nanotube concentration and the volume of the SWNT suspension filtered. The main advantage of this method is its versatility: it could be applied to any other nanoscale fibrous material. By properly adjusting the volume of filtered SWNT suspension, Wu et al. fabricated an ultrathin, transparent, electrically conducting SWNT film (**Figure 2**a).[82] Although the fabrication process

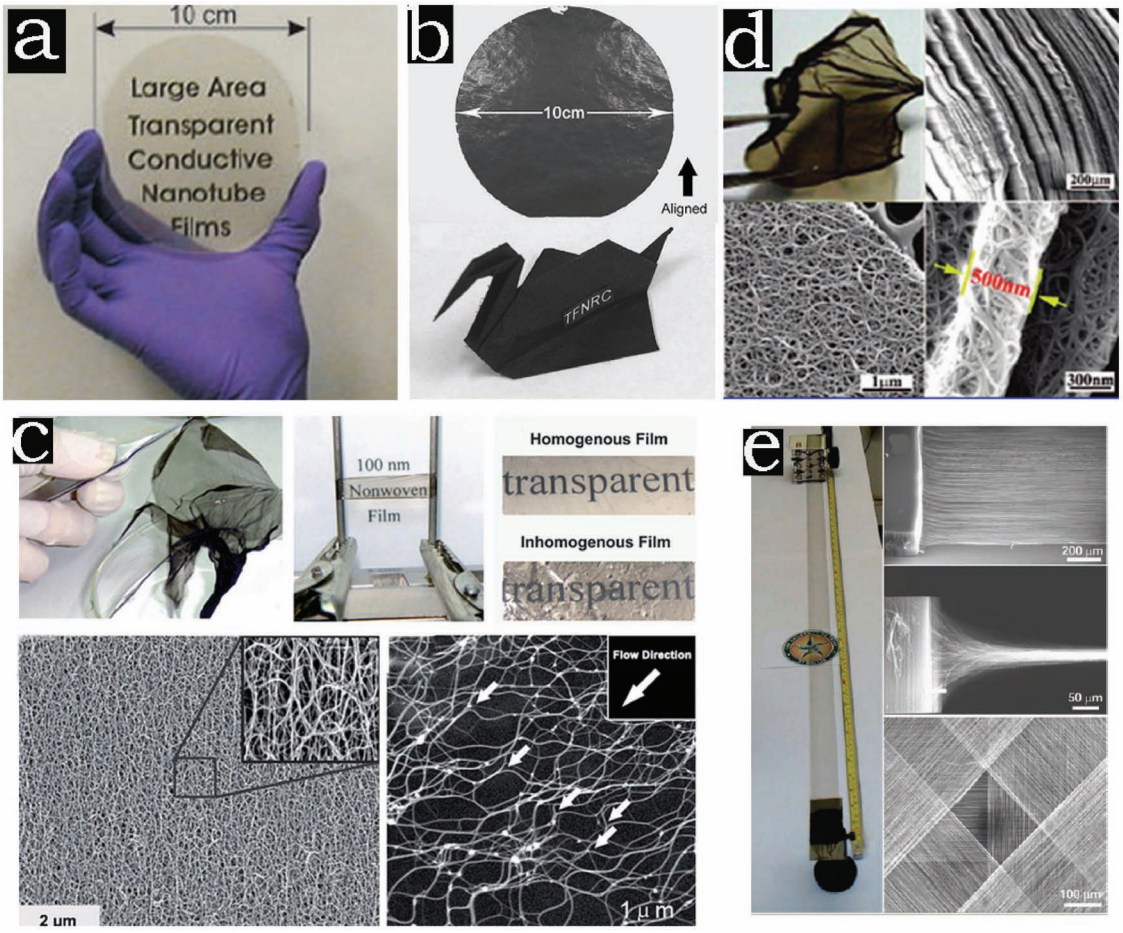

Figure 2. a) Optical image of a transparent, conducting SWNT film on a sapphire substrate. Reproduced with permission from Ref.[82]. Copyright 2004, AAAS. b) Optical image of aligned Bucky paper. Reproduced with permission from Ref.[83]. Copyright 2008, IOP Publishing. c) Optical and SEM images of direct-synthesized SWNT films. Reproduced with permission from Ref.[85]. Copyright 2007, ACS. d) Optical and SEM images of direct-synthesized SWNT films with multilayered structures. Reproduced with permission from Ref.[88]. Copyright 2009 ACS. e) Optical and SEM images of CNT films continuously drawing from aligned CNT array. Reproduced with permission from Ref.[63]. Copyright 2005, AAAS.

for "Bucky paper" is really simple, it must be noted that the vacuum-filtration method also suffers severe limitations in terms of production efficiency and product quality. Therefore, the development of more flexible approaches is desirable.

2.2.2. Unidirectional Bucky Paper from Aligned CNT Arrays

Different from the randomly oriented Bucky paper described above, a simple and effective method called "domino pushing" was recently proposed to fabricate aligned Bucky paper using aligned MWNT arrays as a starting material (Figure 2b).[83] The as received MWNT arrays were forced down in one direction by pushing a cylinder with constant pressure, and thereby all nanotubes in the array were attracted together due to strong van der Waals forces and formed an aligned Bucky paper. The aligned Bucky paper was easily peeled off the membrane after solvent permeation. The axial electical conductivity of Bucky paper was 200 S m^{-1} at room temperature, whereas the value for conventional Bucky paper is 150 S m^{-1}. Such improvement is attributed to the fairly straight nanotubes.

2.2.3. Direct Growth of CNT Films by CVD

CVD is not only an effective way to synthesize bulk CNT powders, but it also provides a direct-growth method to fabricate macroscopic CNT films. Based on their prior work to produce nonwoven SWNT films,[84] Ma et al. recently synthesized strong, highly conducting, transparent, free-standing SWNT films through a modified floating-catalyst CVD (FCCVD) technique. By precisely controlling the sublimation rates of the catalysts as well as the gas flow, different thicknesses of SWNT films with varied transparency were obtained.[85,86] Figure 2c shows the photographs and scanning electron microscope (SEM) images of the as-grown SWNT film. The nanotubes were homogeneously distributed and entangled in the films, and the nanotube bundles were preferentially aligned along the flow direction, forming a Y-type junction. Electrical measurements indicated that the conductivity of the SWNT films could reach up to 2026 S cm^{-1}, which is over 60 times larger than that of unpurified HiPCO (high pressure carbon monoxide) transparent films and nearly 3 times that of purified arc-discharge SWNT films.[87] Such superior electric performance could be attributed to the lower intertube resistance, high purity, and the anisotropic feature of SWTN films. Mechanical tensile tests indicated that the failure strength of the film was 360 MPa, and the Young's modulus around 5 GPa. Recently, Li et al. further advanced this method and fabricated macroscopic SWNT sheets with multilayer structures (Figure 2d). The resulting SWNT sheets showed potential as high-efficiency molecular separation filters and high-capacitance electrodes.[88] Despite the as-produced SWNT sheets having excellent electrical conductivity and mechanical flexibility, however, the as-synthesized SWNT films by FCCVD are still limited by their low yield. Furthermore, the main factors affecting the film morphology and its properties need to be explored and clarified, e.g., carbon source, catalyst, carrier gas, growth rate, substrate, external field, and so on.

2.2.4. Continuous Drawing of MWNT Sheets from Aligned MWNT Arrays

The methods mentioned above are versatile, promising, and cost-effective, however, the main issues regarding the scaled-up fabrication of large-area, free-standing CNT films, including the precise control of film thickness, homogeneity, and film cutting and shaping, have not yet been well resolved. An alternative route toward the mass production of CNT films is to directly draw them from the super-aligned MWNT arrays as shown in Figure 2e.[63] The resulting CNT films have large-scale sizes and anisotropic features, where the constituent CNTs are aligned parallel to one another along the draw direction and form end-to-end jointed connections through the whole film. For example, one silicon wafer of super-aligned MWNT arrays (4 in., where 1 inch ≈ 2.54 cm) was capable of being transformed into a continuous unidirectional CNT sheet 10 cm wide and 100 m long.[48] Besides the batch production of free-standing CNT films, synthesizing CNT films with controlled nanotube structures (e.g., diameter, number of walls, length) to meet a variety of industrial demands is another important issue. Recently, Liu et al. successfully fabricated continuous CNT sheets with tunable optical transmittance, electrical transport, and light emission properties through controlling the tube diameter and length of as-produced MWNT arrays.[89]

2.3. 3D CNT Assemblies

Compared to the randomly tangled CNTs created through arc-discharge or laser-ablation techniques, the fabrication of aligned and oriented CNT structures on certain substrates with macroscopic sizes in 3 dimensions was implemented using CVD.[90–94] So far, even though great progress has been made to grow vertically aligned MWNT arrays, the growth of vertical SWNT arrays is still in an early stage. The dominant issues affecting the fabrication of SWNT arrays are how to maintain the catalytic activity of densely packed catalytic nanoparticles as well as how to remove the amorphous carbon from the catalyst surfaces in order to facilitate SWNT growth. In 2004, a breakthrough was made by Hata et al., in which a water-assisted synthetic CVD approach was developed to grow super-dense, vertically aligned SWNT forests with millimeter-scale height.[95] With the assistance of water vapor, the amorphous carbon coated on the catalyst surfaces was efficiently removed. Accordingly, both the activity and lifetime of the catalyst nanoparticles were dramatically preserved and promoted, thereby facilitating the growth of aligned SWNT arrays. **Figure 3**a,b present the large-scale patterned, highly organized, complex 3D SWNT structures with the assistance of lithographical techniques. Despite considerable efforts made in the synthesis of aligned SWNT arrays, the approach to grow large-scale, highly reproducible, and ultra-high-yield vertical SWNT arrays on any desirable substrate (including metal and plastic) under mild conditions still remains a difficult task. Dai et al. advanced an oxygen-assisted, plasma-enhanced CVD (PE-CVD) method to fabricate aligned SWNT arrays, in which the reactive

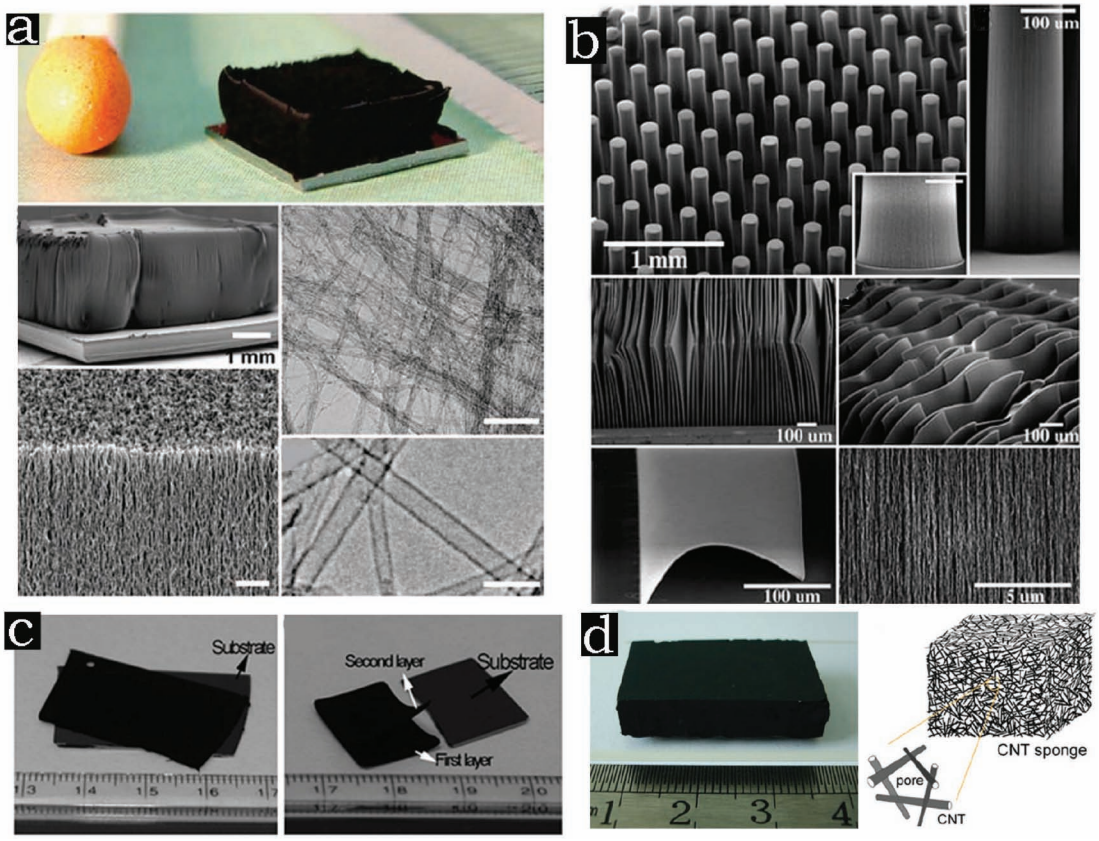

Figure 3. a,b) Optical and electron microscopy images of organized SWNT structures. Reproduced with permission from Ref.[95]. Copyright 2004, AAAS. c) Optical images of free-standing MWNT films with multilayered structures. Reproduced with permission from Ref.[99]. d) Optical image of CNT sponge and its schematic illustration. Reproduced with permission from Ref.[100].

hydrogen species in the chamber was highly scavenged owing to the addition of oxygen to methane during the PE-CVD process.[96] Thus, a C-rich and H-deficient condition would favor the formation of sp^2-like graphitic SWNT structures.

In general, the properties of the supporting substrates on which the CNT arrays are grown play a critical role in some of applications. For instance, CNT arrays on conductive metallic substrates exhibit improved field-emission properties,[97] whereas CNT arrays on flexible polymer substrates might be better suited for certain device applications.[98] In some special cases, the transfer or deposition of nanotube arrays onto a new substrate, rather than the ones they were grown on, was required. Thus, it is desirable to develop a technique to obtain freestanding CNT arrays. Recently, Ci et al. utilized a water-assisted CVD method to grow multilayered, freestanding CNT arrays, in which each single layer could be directly peeled from the substrate without disturbing or degrading the alignment of nanotubes (Figure 3c).[99] Employing similar methods to grow aligned CNT arrays, Gui and co-workers recently fabricated a spongelike CNT material in which nanotubes were randomly interconnected into a 3D framework as show in Figure 3d.[100] In this case, dichlorobenzene was employed as a novel carbon source to disturb the aligned growth of the nanotubes, and thereby nanotubes were consecutively stacked in a random manner to form an interconnected structure with centimeter-scale thickness. The formed CNT sponge, with a porosity of >99%, showed high structural flexibility, robustness, and wettability to organics. By varying the injection rate of carbon the source, the bulk densities of resulting sponges were ranged from 5.8 to 25.5 mg cm^{-3}.[101]

3. Mechanical Properties of CNT Assemblies

3.1. Tensile Properties of CNT Fibers and CNT Films

As a typical form of macroscopic CNT assembly, CNT fibers could maximize the translation of the axial stiffness and strength of individual nanotubes to those of the fibers. Recent progress has proven that the optimized CNT fibers exhibit superior strength (up to 8.8 GPa), stiffness (357 GPa), and fracture energy (121 J g^{-1}), which is considerably greater than any commercial high-strength fibers.[36] This encouraging breakthrough highlights the potential of CNT fibers as structural reinforcing elements in conventional composite fields. It should be pointed out however, that both the reported tensile modulus and strength of CNT fibers by different groups still lies in a wide range of 30–357 GPa and 0.2–8.8 GPa, respectively, no matter whether they are spun from aerogels,[44,45] arrays,[46–50] or suspensions.[54,56,57] Such variation makes it hard for CNT fibers to compete with conventional

high-performance fiber materials (e.g., Kevlar and carbon fibers). Consequently, it is fundamentally important to probe the critical factors affecting the mechanical properties of CNT fibers.

Depending on the starting nanotubes employed as well as the fiber assembling techniques involved, there are two major factors dominating CNT fibers' mechanical behavior, namely, the CNT structures and CNT fiber geometries. Research has confirmed that the nanotube structure (diameter, aspect ratio, defects, morphology, purity, and orientation) imposes an unexceptional influence on the fiber properties. Theoretically, CNTs that are as long and as structurally perfect as possible are ideal candidates to make a high performance fiber. Compared with MWNTs, SWNTs or DWNTs could be made comparatively free of grown-in defects and thereby become the best candidates to achieve good fiber performances. For example, a CNT fiber consisting of mainly DWNTs with an aspect ratio on the order of 10^5 shows the best strength and stiffness 2.2 and 160 N tex^{-1}, respectively (tex is defined as the mass in grams per 1000 meters), and its fracture energy reached 46 J g^{-1}, which exceeds the best commercial available fibers.[51] In addition, the large diameter DWNTs with flattened tubular morphologies tend to maximize the contacting areas, resulting in efficient stress transfer between neighboring nanotubes under tensile loading conditions.

Besides the nanotube structural influences described above, the geometric parameters of the CNT fibers (e.g., diameter, twist angle, and volume fraction) also play an important role in determining the mechanical behavior of the fibers. Twist was normally introduced to a CNT fiber to reduce the spaces between adjacent nanotubes and to increase the density of the fibers. Liu et al. have pointed out that both the tensile strength and Young's modulus would monotonically reduce with increasing twisting angles of MWNT fibers.[50] This implied that a CNT fiber twisted to a larger extent possesses a larger stretchability but a lower strength and modulus. Voids or inclusions would be inevitably introduced into fibers during a fiber-twisting process, and it is difficult to accurately measure the void volume fraction within the fiber. Therefore, researchers started to employ the linear density (g km^{-1}) or specific gravity (the density of the material divided by that of water) to describe the strength or stiffness of CNT fibers.[36] Nevertheless, it should be pointed out that such analyses are based on conventional mechanical tests, by which it is difficult to accurately reflect the individual nanotube contributions to the fiber. Moreover, the discontinuous features of the nanotube elements insides a CNT fiber also impede the effective loading reinforcement due to the shear-lag and, thus, it is necessary to enhance the interbundle connection and the load transfer for CNT fiber at a microscale or nanoscale level. Up to now, a great deal of effort has been made to strengthen CNT bundles via noncovalent and covalent bonding,[55,102] but little attention has been paid to the design of a load-transfer-favored structure. Our recent work has proven that reticulate CNT architectures not only work as continuous load-transfer pathways, but also strongly couple with polymer chains at the molecular level, which results in unique mechanical properties completely different from those of conventional composites (**Figure 4**a).[103] For example, the strengths of epoxy- and poly(vinyl alcohol) (PVA)-infiltrated fibers are notably improved as compared to neat CNT fibers, as represented in Figure 4b. Additionally, our results imply that the molecular-level coupling between reticulate CNT and polymer chains could not only effectively constrain the free deformation of nanotube networks but also greatly enhance the strength of their interbundle connections. The interbundle slippage of CNT fibers is effectively hindered after filling with low-strength epoxy. Consequently, a high tensile strength (close to 1.5 GPa) was observed for epoxy-infiltrated composite fibers. Depending on the infiltrating polymer structure itself, a different coupling role was observed for the PVA-infiltrated composite fibers, where plastic flow of polymer chains occurred for PVA-infiltrated fibers under large strain, and then the concentration of stress was mitigated and the

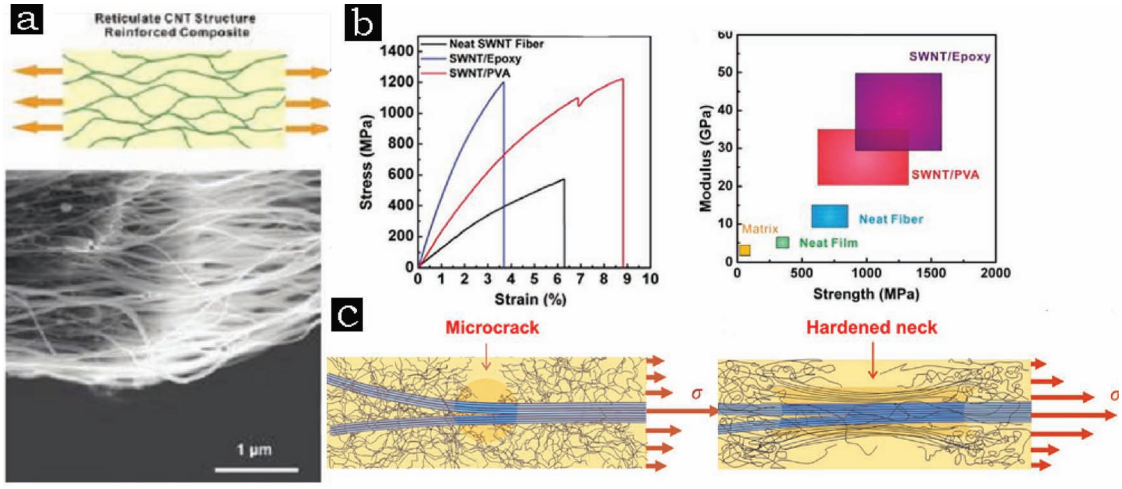

Figure 4. a) Schematic of internal structure of reticulate CNT-reinforced composite, and SEM image of the fracture section for an epoxy-infiltrated composite fiber. b) Typical tensile curves for composite fibers and neat SWNT fibers, and a summary of the tensile modulus and strength for the tested samples. c) Schematic of fracture mechanisms for epoxy- and PVA-infiltrated composite fibers. Reproduced with permission from Ref.[103]. Copyright 2009, ACS.

small NANO MICRO

interbundle junction protected. Finally, the toughness of PVA-infiltrated fibers could reach 50 J g^{-1}, which is far superior to commercially used high-strength fibers such as Kevlar (33 J g^{-1}) or graphite fiber (12 J g^{-1}). Figure 4c shows the schematic illustration of different fracture mechanisms for epoxy- and PVA-infiltrated composite fibers.

In comparison with CNT fibers, the randomly oriented nature of nanotubes as well as the poor van der Waals forces present in the macroscale Bucky paper membranes made the mechanical properties undesirable.[104,105] To create the strong binding force between isolated nanotubes or their bundles, chemical crosslinking of SWNTs by means of electron-beam (e-beam) irradiation was introduced to the Bucky paper membranes. The resulting membranes showed a substantial improvement of mechanical properties without sacrificing the electrical and thermal properties of the nanotubes.[106] Besides the e-beam induced crosslinking approach, a novel and simple method based on filtration was proposed to fabricate CNT-based composite films with a high weight-content of nanotubes. The polymer chains were intercalated into either the pre-existing porous internal structures of nanotube membranes, or partially diffused between individual nanotubes within the ropes.[107] Although these composites showed some reinforcement, their mechanical properties still fell short of those of standard composites.[108] Recently, with the adoption of new processing techniques for composite films, the tensile modulus and strength of buckypaper-based composites has reached 15.4 GPa and 400 MPa, respectively.[109,110] On the basis of layer-by-layer assembly, Kotov et al. fabricated the high weight-loading (around 50 wt%) CNT-based polyelectrolyte composite films. After further chemical crosslinking between the nanotubes and the polymer matrices, the resulting tensile strength of the CNT films could reach 325 MPa.[111,112] Although the poor matrix–nanotube interfacial bonding and phase segregation have been successfully mitigated, similar to the vacuum-filtration method, this fabrication procedure also suffered from poor efficiency and product quality. An alternative route toward CNT-based composite films with superior performances consisted of directly using free-standing 2D CNT sheets. Recently, Cheng et al. fabricated continuous, aligned CNT-sheet-based epoxy composites by a vacuum-assisted resin infiltration method, in which the high nanotube content was well-dispersed and highly oriented.[113] Mechanical measurements have indicated that 347% enhancement of the Young's modulus and 45% enhancement of tensile strength were achieved for 8.1 wt% CNT-based epoxy composites as compared to pure epoxy. Meanwhile, based on the classic rule of mixtures, the derived tensile modulus and the strength of neat CNT sheets were 176 GPa and 746 MPa, respectively, which is much higher than the experimentally measured 40 GPa (modulus) and 643 MPa (strength). This discrepancy implies that the reinforcing mechanism of macroscopic CNT-assembly-based composites might be different from that of the conventional fiber-based composites, which agrees well with our recent reports.[103,114]

3.2. Micromechanical Analysis of the Loading Role of CNT Fibers

To illustrate the reinforcement efficiency of nanotube elements inside CNT fibers as well as to investigate the microscopic failure process of fibers at microscale level, we recently developed a generic methodology independent of conventional mechanical measurements to investigate the load-bearing capability of the nanotubes inside the fiber with the help of in situ Raman-tensile methodology.[59] Since Raman scattering is sensitive to the interatomic distance, when CNTs are mechanically strained, there is a linear relationship between the shift of the Raman peaks and the local strain.[115,116] By investigating the variation of the Raman G′ band under strain, we could infer the structural deformation process of the CNT fibers and, further, predict the macrostructures' moduli (**Figure 5**). The strain transfer factor (STF),

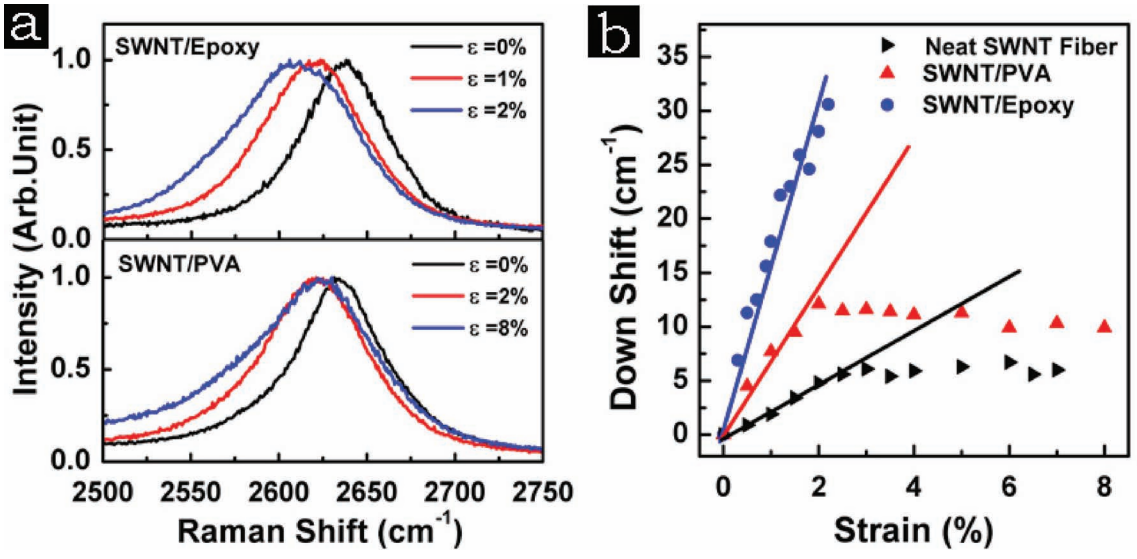

Figure 5. a) Typical Raman G′ bands of epoxy- and PVA-infiltrated composite fibers under a variety of strains. b) Downshifts of the peak position in different systems. Reproduced with permission from Ref.[103]. Copyright 2009, ACS.

defining the ratio of the downshift rate of the G′ band for a strained CNT assembly to the average downshift rate of the G′ band of strained individual CNTs, was proposed to quantitatively evaluate the load-bearing capability of CNT fibers. For example, the STFs for neat CNT fibers, PVA-, and epoxy-infiltrated composite fibers were 0.045, 0.18, and 0.4, respectively, meaning there were improvements of 4 and 9 times on the strain transfer efficiency after the incorporation of epoxy and PVA.[103] Additionally, with the direct link between macroscale strain and the CNTs' axial extension via STF, we further proposed a theoretical formula to predict the modulus of CNTs assemblies after revising the classic rule of mixture.

$$E = \langle \cos^2 \theta \rangle \alpha f E_t + (1 - f) E_m \quad (1)$$

where E, E_t, and E_m refer to the Young's moduli of the CNT fibers, individual nanotubes (in bundles), and polymer respectively; f and α are the volume fraction of nanotubes and STF, respectively; $<\cos^2\theta>$ describes the contribution of the averaged orientation angle of the nanotubes in the continuous network. For neat CNT fibers, the second part of Equation 1 can be neglected. **Table 1** lists the predicted modulus values given by Equation 1 and the experimental results. From this, it can be concluded that the revised rule of mixtures fits the experimental data very well for the $<\cos^2\theta>$ value of 0.4–0.6 in our case. Consequently, based on the shift rate of specific Raman bands at the low strain region, we could predict the modulus of the SWNT macroarchitectures and their composites accurately.

Despite extensive research into the static mechanical properties of CNT fibers for several years, data on the fatigue limits of CNT fibers under both static and dynamic loading conditions have never been reported yet. Recent work has pointed out that the static fatigue strength of CNT fibers is at least twice that of graphite fibers within short times and similar to that of graphite fibers at longer times, while the dynamic fatigue strength is twice that of the graphite fibers up to 10^7 cycles.[117]

3.3. Compressive Behavior of 3D CNT Assemblies

Owing to its small diameter, an individual CNT exhibits extreme structural flexibility and can be repeatedly bent through large angles (e.g., buckling) and strains without structural failure.[118–120] Such remarkable flexibility and resilience of nanotubes potentially make them an ideal low-weight foamlike material once they are organized into specific 3D architectures, such as aligned 3D arrays or foams. Recent work has demonstrated that vertically aligned MWNT arrays exhibit super-compressible behavior, in which individual nanotubes act as strong nanoscale struts and the internanotube spaces act as interconnected open-air cells.[121,122] The compressed nanotubes could be collectively squeezed by buckling and folding themselves like springs. After each cycle of uniaxial compressive loading, the nanotubes can either recover to their near-original lengths or achieve a partial recovery depending on the morphology of the s-received aligned CNT arrays as well as the applied strain level.[123] Compared to conventional low-density flexible foams, the aligned nanotube arrays possessed high compressive strengths (close to 15 MPa), sag factors (≈4), recovery rates (>2000 μm s^{-1}), and breathability, which might be useful in compliant interconnecting structures for mechanical-damping and energy-absorbing services.[121] Interestingly, although the individual nanotube behaviour is essentially elastic, the free-standing nanotube arrays exhibit a nonlinear stress–strain behavior.[124] Fatigue resistance tests under compression indicate that aligned CNT arrays exhibit behaviors that are common features of viscoelastic materials, e.g., preconditioning, hysteresis, nonlinear elasticity, and stress relaxation. A comparison of CNT arrays and other contractile materials indicates that the CNT arrays are comparable to human muscle tissues in terms of their mechanical properties. This combination of soft-tissuelike behaviour and outstanding fatigue resistance of CNT arrays suggests that properly engineered nanotube structures could form artificial tissues.

Similar to the compressible behavior of aligned CNT arrays exhibited, CNT sponges show high structure flexibility and robustness.[100] Experiments have confirmed that the sponges could sustain large strain deformations, recover most of their material volume elastically, and resist structural fatigue under cyclic stress conditions in both air and liquids. Different from the heavy buckles formed along nanotube axes within the CNT arrays, the large-degree compression on these sponges stemmed from the squeezing of intertube pores. Furthermore, the CNT sponges exhibit isotropic compressive behavior when tested in different directions. The compressibility of CNT sponges shows dependence on the material density as well as on the applied compressive stress. For instance, the compressive strength consistently increased by 20 times when the sponge density changed from 5.8 to 25.5 mg cm^{-3}.[101] Anyway, it should be noted that all of the sponges showed very low Young's moduli (<0.1 MPa) as compared to aligned CNT arrays.

Table 1. Comparison of the Predicted Modulus Values for Various SWNT Fibers with Experimental Results (Reproduced with permission from Ref.[103]. Copyright 2009, ACS)

Specimens	Volume fraction (f)	STF (α)	Predicted modulus [GPa]				Experimental modulus [GPa]
			$<\cos^2\theta> = 1/3$	$<\cos^2\theta> = 0.4$	$<\cos^2\theta> = 0.5$	$<\cos^2\theta> = 0.6$	
SWNT fiber	0.65 ~ 0.75	0.045	6 ~ 7	7 ~ 9	9 ~ 11	11 ~ 13	9 ~ 15
Epoxy–SWNT	0.3 ~ 0.4	0.4	27 ~ 36	32 ~ 43	40 ~ 53	48 ~ 63	30 ~ 50
PVA–SWNT	0.4 ~ 0.5	0.18	17 ~ 21	19 ~ 25	24 ~ 31	29 ~ 37	20 ~ 35

NANO MICRO small

4. Applications of CNT Assemblies

4.1. Structural Reinforcing Fillers in Conventional Composites Based on CNT Fibers

Thus far the direct use of CNT powders in polymer composites for structural reinforcement has been disappointing due to unoptimized parameters such as dispersion, alignment, and interfacial properties.[19,21,22,125] Motivated by the mass production of high performance CNT fibers,[36] Mora et al. fabricated high volume-fraction (>25%) CNT-fiber-based epoxy composites. The reinforcement efficiency of the CNT-fiber-incorporated composites was similar to that of standard composites reinforced with commercial carbon fibers. Surprisingly, the CNT fibers also performed well as reinforcement in compressive modes, which is unusual in the conventional high-strength fiber based composites.[126] With the help of in-situ Raman spectroscopy, we recently proved that the stiffening and strengthening roles of CNT fibers inside polymeric matrices are determined by nanotube elements.[114] In such cases, the molecular coupling between nanotubes and polymer chains effectively impedes the initiation of nanotubes buckling at lower compressive strains. Thus, the CNT fibers behave with notable flexibility without permanent deformation or failure under compressive stress. That is to say, CNT fibers combine superior stiffening, strengthening, and flexibility that would meet various demands for next-generation advanced composites.

4.2. Optoelectronics and Electrochemical Devices Based on 2D CNT Films

As an essential element of antistatic coatings, flat panel displays, organic light-emitting diodes,[87,127,128] solar cells,[70–72] and electrochromic devices,[129] indium tin oxide (ITO) has been widely used as a transparent conductor. Unfortunately, its intrinsic brittleness, the limited availability of indium, and its chemical instability to corrosion greatly limits its further applications, particularly in mechanically flexible-substrate-based electronic systems. Recently, thin transparent CNT films have received increased attention as replacement conductive materials owing to their attractive electrical, optical, and mechanical properties and their stretchability and chemical stability.[74,75,130] To date, encouraging progress has been made in the scaling-up of their fabrication and in the application of transparent conductive CNT-based films.[74,75,131] For example, Rogers et al. fabricated the high-performance "all-tube"-constructed flexible, transparent transistors with an effective mobility ≈ 30 $cm^2 V^{-1} s^{-1}$ and a high mechanical stretchability (<3.5%).[132] As shown in **Figure 6**a, owing to the relatively high work function of SWNT films (≈4.9 eV),[133] they can serve as anodes for hole-injection/extraction in organic light-emitting diodes (OLEDs) and organic photovoltaic devices (Figure 6b,c).[70,87] Results have demonstrated that the luminescence, turn-on voltages, and power efficiencies of CNT-based devices are comparable to those of devices with ITO electrodes.[61,62,126] Encouragingly, CNT-film-based integrated digital circuits and transistor radios have been successfully constructed (Figure 6d,e).[73,134] Furthermore, because of the high accessible surface area of porous nanotube morphology, in combination with their high electrical conductivity, low mass density, and chemical stability, non-transparent CNT-based sheets are also attractive candidates for a variety of energy-conversion and storage technologies (Figure 6f–h).[66–68,135–137] Examples include 'supercapacitors', which give giant capacitances in comparison with those of ordinary dielectric-based capacitors. So far, driven by its promising high power density,[138] CNT-based supercapacitors have not only achieved notable energy and power performances,[66] they have also enabled new functionalities, providing flexible, stretchable, and transparent supercapacitors.[67,139,140] Even though these studies have shown advantageous individual properties of CNTs for supercapacitors, a comprehensive demonstration of their full potential as electrodes meeting all relevant criteria for practical devices has yet to be presented. Recently, Izadi-Najafabadi et al. investigated the full potential of SWNT-based super-capacitor electrodes using aligned SWNT arrays as starting-material (Figure 6f).[141] The energy density and maximum power density of the SWNT electrodes could reach 94 Wh kg^{-1} and 210 kW kg^{-1}, respectively, which surpasses most other CNT electrodes reported. Aside from the performance of CNT-based supercapacitors, fabrication methods for CNT-based energy-storage devices would also influence the development and application of these lightweight electronics. Therefore, innovation to manufacture the scalable, low-cost, stretchable, and highly conductive CNT-based energy devices to meet the technology demands of modern society is another daunting challenge. With the help of simple solution-processing (e.g., conformal coating, dipping, and drying), Hu et al. have successfully fabricated CNT-based commercial paper or textile energy devices (Figure 6g,h), which will bring new opportunities for advanced applications in energy storage and conversion.[66–68] In addition, the CNT-sheet supercapacitors are able to retain charge in the absence of contacting electrolyte, which greatly extends their charge-storage times and is of significant importance in various applications.[142] Nevertheless, different from the promising applications of transparent CNT films prepared through the solution-processing and/or printing procedures described above, it is important to note that the potentials of CNT films fabricated by the direct CVD approach in the electronics and optoelectronics fields are still on the way.

4.3. Miscellaneous Applications of 3D CNT Arrays

So far, even though the reinforcement of randomly dispersed CNT-based composites has been disappointing in most cases, these 3D CNT arrays are able to shed light on the potential of conventional composite fields in a very different way. Recently, Ajayan and co-workers demonstrated that 3D CNT arrays directly grown onto the surface of microfiber SiC fabrics (**Figure 7**a) can act as building blocks to improve the interlaminar strength and toughness of conventional 3D multilayered composites without compromising their in-plane properties.[143] Afterward, a versatile approach based

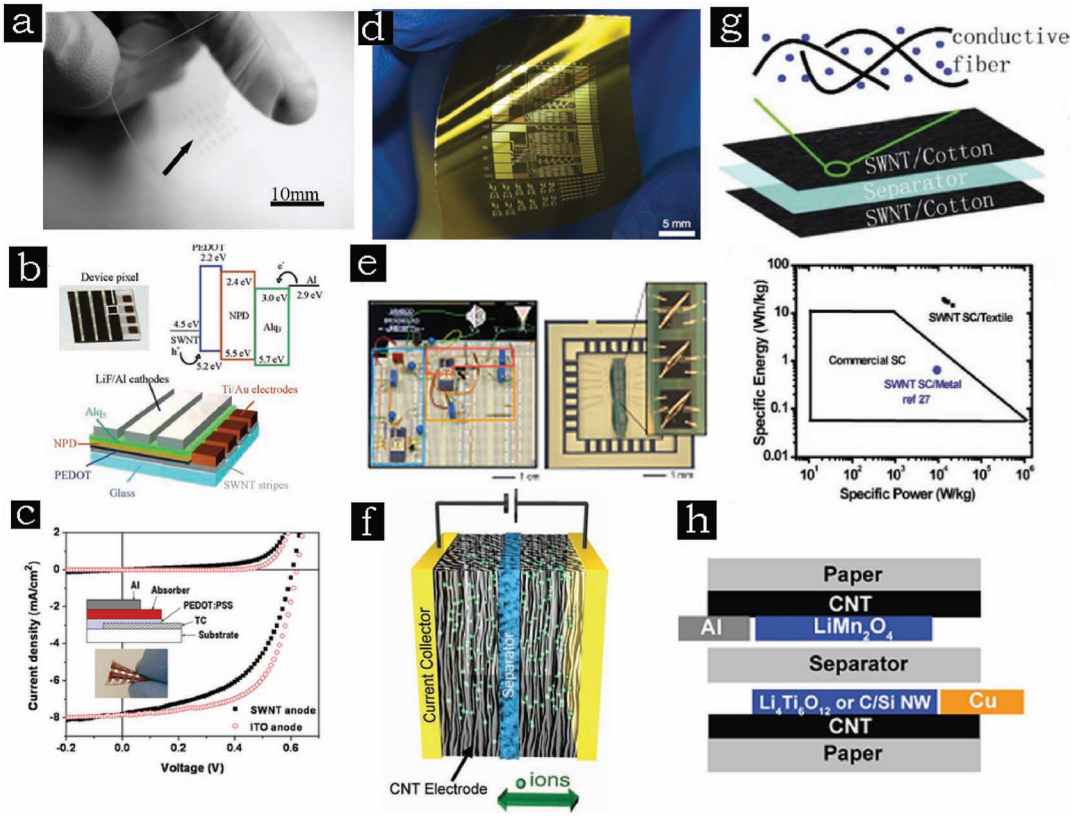

Figure 6. a) An array of 'all-tube' flexible transparent TFTs on a plastic substrate. Reproduced with permission from Ref.[132]. b) Schematic OLED device of patterned CNT as electrode. Inset: photograph of a single device fabricated on glass. Reproduced with permission from Ref.[87]. Copyright 2006, ACS. c) Current density–voltage curves for organic solar cells using ITO or SWNT thin films as anodes. Inset: schematic of device and photograph of flexible cell using SWNT on PET. Reproduced with permission from Ref.[70]. Copyright 2006, American Institute of Physics. d) Flexible SWNT integrated-circuit chip bonded to a curved surface. Reproduced with permission from Ref.[73]. Copyright 2008, Nature Publishing Group. e) Radio system, with magnified view of SWNT-transistor wire bonded into a package. Reproduced with permission form Ref.[134]. Copyright 2008, The National Academy of Science. f) Schematic of typical cell assembly. Reproduced with permission from Ref.[141]. g) Schematic supercapacitor with porous SWNT textile conductor as the electrodes and current collectors and its cycling stability. Reproduced with permission from Ref.[67]. Copyright 2010, ACS. h) Schematic of SWNT conductive paper as the current collector for a Li-ion battery. Reproduced with permission from Ref.[66]. Copyright 2009, The National Academy of Science.

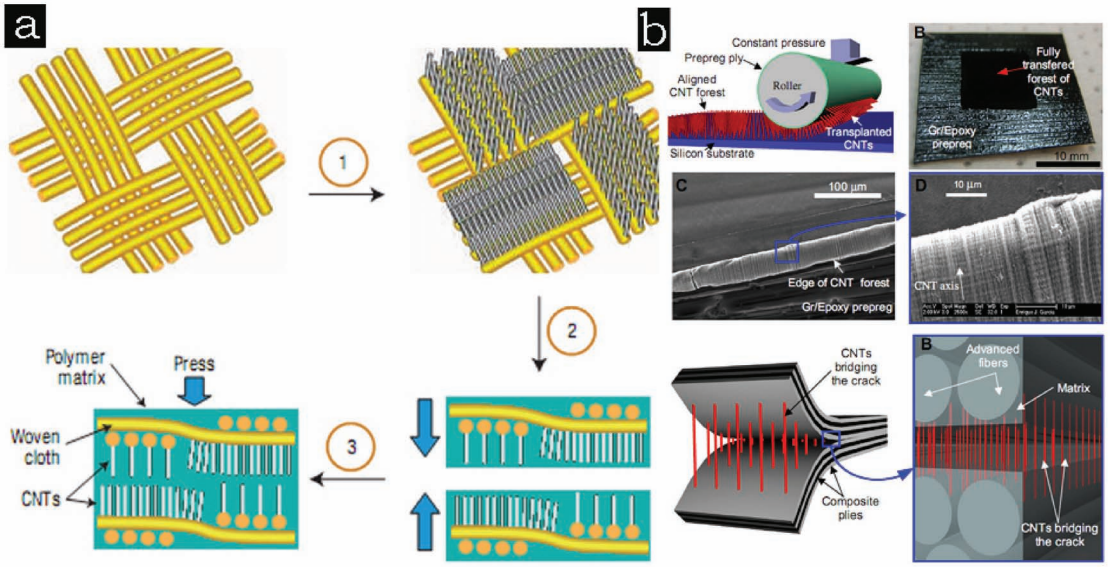

Figure 7. a) Schematics of the steps involved in the nanomanufacturing of CNT-array-based 3D composites. Reproduced with permission from Ref.[143]. Copyright 2006, Nature Publishing Group. b) Transfer-printing of CNT array to prepreg and illustration of toughening role. Reproduced with permission from Ref.[144]. Copyright 2008, Elsevier.

NANO MICRO small

on 'transfer-printing' was developed to transplant an aligned CNT array from its original substrate to any desired surface, e.g., carbon tape prepreg—a reinforcing material combined with a full complement of resin before the molding operation (Figure 7b). An improvement to the fracture toughness of around 1.5–3 times was reported for CNT-modified composite laminates, owing to the bridging effects of nanotubes between adjacent layers.[144] In addition, the 3D CNT array grafted onto the microscale fibre ends (e.g., SiC) could also be used to make multifunctional, conductive brushes. These tiny brushes with nanotube bristles have been demonstrated for use in a variety of applications including the cleaning of microscale spaces, conducting contact brushes, and probe arrays.[145]

Besides being promising candidates in conventional 3D composites, another interesting application that has been touted for 3D CNT arrays is their use as membrane filters. In comparison with traditional activated and porous carbon filters, the uniform nanoscale pore size of CNT arrays could allow them to act as small-molecule separation filters.[29–33] Even with the small diameter of individual nanotubes, the flux through the tubes was high due to the smoothness of the CNT walls.[146] After chemical modification of the CNT surface, the CNT arrays were able to filter selectively. Instead of utilizing open-ended CNT pores as transport pathways, Srivastava et al. advanced CNT-array-based filters by directly utilizing the interstitial spaces between CNTs, which showed potential for the filtration of heavier hydrocarbon species from hydrocarboneus oil.[147] Through properly tuning the porosity of aligned CNT arrays by applying different levels of mechanical compression, the nanotube membranes also performed efficient filtration of a series of protein molecules with various molecular weights.[148] To fully utilize the high nanoscale porosity of CNT arrays, Yu et al. fabricated high-porosity (≈20%), free-standing CNT membranes by means of a solvent-evaporation-based shrinking method, after which the diameter of both the CNTs and interstitial pores were approximately 3 nm.[149] Since no polymer filler was incorporated, gases permeated efficiently through the nanotubes as well as the interstitial spaces. Consequently, the reported gas permeability was 4–7 orders of magnitude higher than that reported in the literature.

5. Conclusion and Outlook

Over the past few years, CNTs have evolved into one of the most intensively studied materials. Today, the bulk volumes of manufactured MWNTs reach a few hundred tons per year, though few applications based on CNTs have indeed been commercialized. The best examples of present bulk applications of CNTs are the use of CVD-grown MWNTs in lithium-ion batteries and in plastics for electrostatic discharge applications. It is important to note that neither of these applications utilize the spectacular mechanical or electrical properties of the nanotubes, which function as additives to add value to the products. Nevertheless, there has been growing interest in the development of various CNT-based polymer composites. In some cases, the performance of such composites at low weight-contents outperforms corresponding conventional carbon-fiber-based composites. Certainly, owing to the high costs as well as the complicated fabrication methods of these composites, they will not be commercialized and utilized in the foreseeable future. Thus, there exist great challenges to transfer the spectacular properties of individual CNTs—in particular, their mechanical and electrical properties—into macroscopic forms. Encouragingly, in the past few years, various macroscopic CNT assemblies have shed light on the maximum utilization of the remarkable properties of individual nanotubes in a wide range of application fields. Examples include super-strong 1D CNT fibers, highly flexible 2D-nanotube-sheet-based transparent electronics, super-compressible 3D CNT foams, and so on. The macroscale CNT assemblies have the advantage of easy handling and use under various conditions. Furthermore, the CNT assemblies also exhibit unusual multifunctionalities combining the electrical, mechanical, optical, and chemical properties and, at same time, possess impressive novel behaviors arising from their unique structures. Such CNT assemblies as alternative materials have shown various potential applications such as high-performance composites for aircraft and automotive industries, electronics (e.g., flexible electrodes in displays, antistatic coatings, organic light-emitting diodes), energy-storage devices, filters, and biomimic adhesives.

In spite of this progress, significant challenges remain, especially with certain material aspects. First, advanced techniques and novel approaches are imperative for the fabrication of various forms of macroscopic CNT assemblies on a large scale. Second, and perhaps most importantly, not only the processing parameters but also the geometry parameters of nanotube assemblies need to be optimized to achieve superior performance. Third, some of the unusual properties and potential applications of CNT assemblies need further exploration. Nevertheless, in our view, recent progress shows that CNT assemblies offer a unique combination of properties, and outperform conventional materials. Optimization of the performance, the stability of properties, manufacturability, mass production, and the cost of CNT assemblies will ultimately determine the success of these types of materials.

Acknowledgements

This project was jointly supported by the National Key Basic Research Program of China (Grant No. 2007CB936803) and a key international collaboration project (Grant No. 2008DFA51220) of the Ministry of Science and Technology of China, a key item of the Knowledge Innovation Project of the Chinese Academy of Sciences (Grant No. KJCX2-YW- M01), and the National Natural Science Foundation of China (Grant Nos. 20874023, 50753003, and 51073044).

[1] M. Endo, M. S. Strano, P. M. Ajayan in *Carbon Nanotubes: Advanced Topics in the Synthesis, Structure, Properties, and Applications* (Eds. A. Jorio, G. Dresselhaus, M. S. Dresselhaus), Springer, Berlin **2008**, pp.13–62.

[2] P. J. F. Harris, *Carbon Nanotubes and Related Structures: New Materials for the 21st Century*, Cambridge University Press, Cambridge, UK **1999**, pp.111–151.
[3] R. H. Baughman, A. A. Zakhidov, W. A. de Heer, *Science* **2002**, *297*, 787.
[4] C. Dekker, *Phys. Today* **1999**, *52*, 22.
[5] A. Javey, J. Guo, Q. Wang, M. Lundstrom, H. Dai, *Nature* **2003**, *424*, 654.
[6] P. L. MuEuen, M.S. Fuhrer, H.K. Park, *IEEE Transact. Nanotechnol.* **2002**, *1*, 78.
[7] F. Kreupl, A. P. Graham, M. Liebau, G. S. Duesberg, R. Seidel, E. Unger, *IEDM* **2004**, *17*, 683.
[8] Z. Yao, C. L. Kane, C. Dekker, *Phys. Rev. Lett.* **2000**, *84*, 2941.
[9] M. Radosavljevi , J. Lefebvre, A. T. Johnson, *Phys. Rev. B* **2001**, *64*, 241307.
[10] X. Zhou, J. Y. Park, S. Huang, J. Liu, P. L. McEuen, *Phys. Rev. Lett.* **2005**, *95*, 146805.
[11] P. Avouris, Z. Chen, V. Perebeinos, *Nat. Nanotechnol.* **2007**, *2*, 605.
[12] M. F. Yu, B. S. Files, S. Arepalli, R. S. Ruoff, *Phys. Rev. Lett.* **2000**, *84*, 5552.
[13] M. F. Yu, O. Lourie, M. J. Dyer, K. Moloni, T. F. Kelly, R. S. Ruoff, *Science* **2000**, *28*, 637
[14] E. W. Wong, P. E. Sheehan, C. M. Lieber, *Science* **1997**, *277*, 1971.
[15] E. Pop, D. Mann, Q. Wang, K. Goodson, H. Dai, *Nano Lett.* **2006**, *6*, 96.
[16] H. Huang, C. Liu, Y. Wu, S. Fan, *Adv. Mater.* **2005**, *17*, 1652.
[17] K. Kordás, G. Tóth, P. Moilanen, M. Kumpumäki, J. Vähäkangas, A. Uusimäki, R. Vajtai, P. M. Ajayan, *Appl. Phys. Lett.* **2007**, *90*, 123105.
[18] L. S. Schadler in *Nanocomposite Science and Technology*, Wiley-VCH, Weinheim, Germany **2003**, pp.77–153.
[19] P. M. Ajayan, J. M. Tour, *Nature* **2007**, *447*, 1066.
[20] J. N. Coleman, U. Khan, Y. K. Gun'ko, *Adv. Mater.* **2006**, *18*, 689.
[21] M. Moniruzzaman, K. I. Winey, *Macromolecules* **2006**, *39*, 5194.
[22] E. T. Thostenson, Z. Ren, T. W. Chou, *Compos. Sci. Technol.* **2001**, *61*, 1899.
[23] S. Kumar, T. D. Dang, F. E. Arnold, A. R. Bhattacharyya, B. G. Min, X. Zhang, R. A. Vaia, C. Park, W. W. Adams, R. H. Hauge, R. E. Smalley, S. Ramesh, P. A. Willis, *Macromolecules* **2002**, *35*, 9039.
[24] A. B. Dalton, S. Collins, E. Muñoz, J. M. Razal, Von H. Ebron, J. P. Ferraris, J. N. Coleman, B. G. Kim, R. H. Baughman *Nature* **2003**, *423*, 703.
[25] L. Xiao, Z. Chen, C. Feng, L. Liu, Z. Q. Bai, Y. Wang, L. Qian, Y. Zhang, Q. Li, K. Jiang, S. Fan, *Nano Lett.* **2008**, *8*, 4539.
[26] A. E. Aliev, J. Oh, M. E. Kozlov, A. A. Kuznetsov, S. Fang, A. F. Fonseca, R. Ovalle, M. D. Lima, M. H. Haque, Y. N. Gartstein, M. Zhang, A. A. Zakhidov, R. H. Baughman, *Science* **2009**, *323*, 1575.
[27] L. Qu, L. Dai, M. Stone, Z. Xia, Z. L. Wang, *Science* **2008**, *322*, 238.
[28] B. Yurdumakan, N. R. Raravikar, P. M. Ajayan, A. Dhinojwala, *Chem. Commun.* **2005**, 3799.
[29] M. A. Shannon, P. W. Bohn, M. Elimelech, J. G. Georgiadis, B. J. Mariñas, A. M. Mayes, *Nature* **2008**, *452*, 301.
[30] B. J. Hinds, N. Chopra, T. Rantell, R. Andrews, V. Gavalas, L. G. Bachas, *Science* **2004**, *303*, 62.
[31] S. Kim, J. R. Jinschek, H. Chen, D. S. Sholl, E. Marand, *Nano Lett.* **2007**, *7*, 2806.
[32] J. K. Holt, H. G. Park, Y. Wang, M. Stadermann, A. B. Artyukhin, C. P. Grigoropoulos, A. Noy, O. Bakajin, *Science* **2006**, *312*, 1034.
[33] M. Mauter, M. Elimelech, *Environ. Sci. Technol.* **2008**, *42*, 5843.
[34] Z. P. Yang, L. Ci, J. A. Bur, S. Y. Lin, P. M. Ajayan, *Nano Lett.* **2008**, *8*, 446.
[35] R. Haggenmueller, H. H. Gommans, A. G. Rinzler, J. E. Fischer, K. I. Winey, *Chem. Phys. Lett.* **2000**, *330*, 219.
[36] K. Koziol, J. Vilatela, A. Moisala, M. Motta, P. Cunniff, M. Sennett, A. Windle, *Science* **2007**, *318*, 1892.
[37] X. H. Zhong, Y. L. Li, Y. K. Liu, X. H. Qiao, Y. Feng, J. Liang, J. Jin, L. Zhu, F. Hou, J. Y. Li, *Adv. Mater.* **2009**, *22*, 692.
[38] T. Mirfakhrai, J. Oh, M. Kozlov, E. C. W. Fok, M. Zhang, S. Fang, R. H. Baughman, J. D. W. Madden, *Smart. Mater. Struct.* **2007**, *16*, S243.
[39] J. Wei, H. Zhu, D. Wu, B. Wei, *Appl. Phys. Lett.* **2004**, *84*, 4869.
[40] T. W. Chou, L. Gao, E. T. Thostenson, Z. Zhang, J. H. Byun, *Compos. Sci. Technol.* **2010**, *70*, 1.
[41] H. M. Cheng, F. Li, X. Sun, S. D. M. Brown, M. A. Pimenta, A. Marucci, G. Dresselhaus, M. S. Dresselhaus, *Chem. Phys. Lett.* **1998**, *289*, 602.
[42] C. Liu, H. M. Cheng, H. T. Cong, F. Li, G. Su, B. L. Zhou, M. S. Dresselhaus, *Adv. Mater.* **2000**, *12*, 1190.
[43] H. W. Zhu, C. L. Xu, D. H. Wu, B. Q. Wei, R. Vajtai, P. M. Ajayan, *Science* **2002**, *296*, 884.
[44] Y. L. Li, I. A. Kinloch, A. H. Windle, *Science* **2004**, *304*, 276.
[45] M. Motta, Y. L. Li, I. Kinloch, A. Windle, *Nano Lett.* **2005**, *5*, 1529.
[46] K. Jiang, Q. Li, S. Fan, *Nature* **2002**, *419*, 801.
[47] M. Zhang, K. R. Atkinson, R. H. Baughman, *Science* **2004**, *306*, 1358.
[48] X. Zhang, K. Jiang, C. Feng, P. Liu, L. Zhang, J. Kong, T. Zhang, Q. Li, S. Fan, *Adv. Mater.* **2006**, *18*, 1505.
[49] X. Zhang, Q. Li, Y. Tu, Y. Li, J. Y. Coulter, L. Zheng, Y. Zhao, Q. Jia, D. E. Peterson, Y. Zhu, *Small* **2007**, *3*, 244.
[50] K. Liu, Y. Sun, R. Zhou, H. Zhu, J. Wang, L. Liu, S. Fan, K. Jiang, *Nanotechnology* **2010**, *21*, 045708.
[51] M. Motta, A. Moisala, I. A. Kinloch, A. H. Windle, *Adv. Mater.* **2007**, *19*, 3721.
[52] C. D. Tran, W. Humphries, S. M. Smith, C. Huynh, S. Lucas, *Carbon* **2009**, *47*, 2662.
[53] V. A. Davis, L. M. Ericson, A. N. G. Parra-Vasquez, H. Fan, Y. Wang, V. Prieto, J. A. Longoria, S. Ramesh, R. K. Saini, C. Kittrell, W. E. Billups, W. Wade Adams, R. H. Hauge, R. E. Smalley, M. Pasquali, *Macromolecules* **2004**, *37*, 154.
[54] L. M. Ericson, H. Fan, H. Peng, V. A. Davis, W. Zhou, J. Sulpizio, Y. Wang, R. Booker, J. Vavro, C. Guthy, A. N. G. Parra-Vasquez, M. J. Kim, S. Ramesh, R. K. Saini, C. Kittrell, G. Lavin, H. Schmidt, W. W. Adams, W. E. Billups, M. Pasquali, W. F. Hwang, R. H. Hauge, J. E. Fischer, R. E. Smalley, *Science* **2004**, *305*, 1447.
[55] B. Vigolo, A. Pénicaud, C. Coulon, C. Sauder, R. Pailler, C. Journet, P. Bernier, P. Poulin, *Science* **2000**, *290*, 1331.
[56] V. A. Davis, A. N. G. Parra-Vasquez, M. J. Green, P. K. Rai, N. Behabtu, V. Prieto, R. D. Booker, J. Schmidt, E. Kesselman, W. Zhou, H. Fan, W. W. Adams, R. H. Hauge, J. E. Fischer, Y. Cohen, Y. Talmon, R. E. Smalley, M. Pasquali, *Nat. Nanotechnol.* **2009**, *4*, 830.
[57] S. Zhang, K. K. K. Koziol, I. A. Kinloch, A. H. Windle, *Small* **2008**, *4*, 1217.
[58] M. E. Kozlov, R. C. Capps, W. M. Sampson, Von H. Ebron, J. P. Ferraris, R. H. Baughman, *Adv. Mater.* **2005**, *17*, 614.
[59] W. Ma, L. Liu, R. Yang, T. Zhang, Z. Zhang, L. Song, Y. Ren, J. Shen, Z. Niu, W. Zhou, S. Xie, *Adv. Mater.* **2009**, *21*, 603.
[60] G. Liu, Y. Zhao, K. Deng, Z. Liu, W. Chu, J. Chen, Y. Yang, K. Zheng, H. Huang, W. Ma, L. Song, H. Yang, C. Gu, G. Rao, C. Wang, S. Xie, L. Sun, *Nano Lett.* **2008**, *8*, 1071.
[61] Z. Liu, K. Zheng, L. Hu, J. Liu, C. Qiu, H. Zhou, H. Huang, H. Yang, M. Li, C. Gu, S. Xie, L. Qiao, L. Sun, *Adv. Mater.* **2010**, *22*, 999.
[62] L. Ci, Ni. Punbusayakul, J. Wei, R. Vajtai, S. Talapatra, P. M. Ajayan, *Adv. Mater.* **2007**, *19*, 1719.
[63] M. Zhang, S. Fang, A. A. Zakhidov, S. B. Lee, A. E. Aliev, C. D. Williams, K. R. Atkinson, R. H. Baughman, *Science* **2005**, *309*, 1215.

[64] E. S. Snow, F. K. Perkins, E. J. Houser, S. C. Badescu, T. L. Reinecke, *Science* **2005**, *307*, 1942.
[65] E. S. Snow, F. K. Perkins, J. A. Robinson, *Chem. Soc. Rev.* **2006**, *35*, 790.
[66] L. Hu, J. W. Choi, Y. Yang, S. Jeoung, F. L. Mantia, L. F. Cui, Y. Cui, *Proc. Natl. Acad. Sci. USA* **2009**, *106*, 21490.
[67] L. Hu, M. Pasta, F. L. Mantia, L. F. Cui. S. Jeong, H. D. Deshazer, J. W. Chok, S. M. Han, Y. Cui, *Nano Lett.* **2010**, *10*, 708.
[68] L. Hu, H. Wu, Y. Cui, *Appl. Phys. Lett.* **2010**, *96*, 183502.
[69] K. Besteman, J. O. Lee, F. G. M. Wiertz, H. A. Heering, C. Dekker, *Nano Lett.* **2003**, *3*, 727.
[70] M. W. Rowell, M. A. Topinka, M. D. McGehee, H. J. Prall, G. Dennler, N. S. Sariciftci, L. Hu G. Grüner, *Appl. Phys. Lett.* **2006**, *88*, 233506.
[71] J. van de Lagemaat, T. M. Barnes, G. Rumbles, S. E. Shaheen, T. J. Coutts, C. Weeks, I. Levitsky, J. Peltola, P. Glatkowski, *Appl. Phys. Lett.* **2006**, *88*, 233503.
[72] A. D. Pasquier, H. E. Unalan, A. Kanwal, S. Miller, M. Chhowalla, *Appl. Phys. Lett.* **2005**, *87*, 203511.
[73] Q. Cao, H. S. Kim, N. Pimparkar, J. P. Kulkarni, C. Wang, M. Shim, K. Roy, M. A. Alam, J. A. Rogers, *Nature* **2008**, *454*, 495.
[74] Q. Cao, J. A. Rogers, *Adv. Mater.* **2009**, *21*, 29.
[75] G. Grüner, *J. Mater. Chem.* **2006**, *16*, 3533.
[76] H. W. Zhu, B. Q. Wei, *J. Mater. Sci. Technol.* **2008**, *24*, 447.
[77] M. C. LeMieux, M. Roberts, S. Barman, Y. W. Jin, J. M. Kim, Z. Bao, *Science* **2008**, *321*, 101.
[78] R. Duggal, F. Hussain, M. Pasquali, *Adv. Mater.* **2006**, *18*, 29.
[79] X. Li, L. Zhang, X. Wang, I. Shimoyama, X. Sun, W. S. Seo, H. Dai, *J. Am. Chem. Soc.* **2007**, *129*, 4890.
[80] H. Z. Geng, K. K. Kim, K. P. So, Y. S. Lee, Y. Chang, Y. H. Lee, *J. Am. Chem. Soc.* **2007**, *129*, 7758.
[81] J. Liu, A. G. Rinzler, H. Dai, J. H. Hafner, R. K. Bradley, P. J. Boul, A. Lu, T. Iverson, K. Shelimov, C. B. Huffman, F. Rodriguez-Macias, Y. S. Shon, T. R. Lee, D. T. Colbert, R. E. Smalley, *Science* **1998**, *280*, 1253.
[82] Z. Wu, Z. Chen, X. Du, J. M. Logan, J. Sippel, M. Nikolou, K. Kamaras, J. R. Reynolds, D. B. Tanner, A. F. Hebard, A. G. Rinzler, *Science* **2004**, *305*, 1273.
[83] D. Wang, P. Song, C. Liu, W. Wu, S. Fan, *Nanotechnology* **2008**, *19*, 075609.
[84] L. Song, L. Ci, L. Lv, Z. Zhou, X. Yan, D. Liu, H. Yuan. Y. Gao, J. Wang, L. Liu, X. Zhao, Z. Zhang, X. Dou, W. Zhou, G. Wang, S. Xie, *Adv. Mater.* **2004**, *16*, 1529.
[85] W. Ma, L. Song, R. Yang, T. Zhang, Y. Zhao, L. Sun, Y. Ren, D. Liu, L. Liu, J. Shen, Z. Zhang, Y. Xiang, W. Zhou, S. Xie, *Nano Lett.* **2007**, *7*, 2307.
[86] W. Zhou, X. Bai, E. Wang, S. Xie, *Adv. Mater.* **2009**, *21*, 4565.
[87] D. Zhang, K. Ryu, X. Liu, E. Polikarpov, J. Ly, M. E. Tompson, C. Zhou, *Nano Lett.* **2006**, *6*, 1880.
[88] Q. Liu, W. Ren, D. W. Wang, Z. G. Chen, S. Pei, B. Liu, F. Li, H. Cong, C. Liu, H. M. Cheng, *ACS Nano* **2009**, *3*, 707.
[89] K. Liu, Y. Sun, L. Chen, C. Feng, X. Feng, K. Jiang, Y. Zhao, S. Fan, *Nano Lett.* **2008**, *8*, 700.
[90] W. Z. Li, S. S. Xie, L. X. Qian, B. H. Chang, B. S. Zou, W. Y. Zhou, R. A. Zhao, G. Wang, *Science* **1996**, *274*, 1701.
[91] Z. F. Ren, Z. P. Huang, J. W. Xu, J. H. Wang, P. Bush, M. P. Siegal, P. N. Provencio*Science* **1998**, *282*, 1105.
[92] S. Fan, M. G. Chapline, N. R. Franklin, T. W. Tombler, A. M. Cassell, H. Dai*Science* **1999**, *283*, 512.
[93] B. Q. Wei, R. Vajtai, Y. Jung, J. Ward, R. Zhang, G. Ramanath, P. M. Ajayan, *Nature* **2002**, *416*, 495.
[94] R. Andrews, D. Jacques, A. M. Rao, F. Derbyshire, D. Qian, X. Fan, E. C. Dickey, J. Chen *Chem. Phys. Lett.* **1999**, *303*, 467.
[95] K. Hata, D. N. Futaba, K. Mizuno, T. Namai, M. Yumura, S. Iijima, *Science* **2004**, *306*, 1362.
[96] G. Zhang, D. Mann, L. Zhang, A. Javey, Y. Li, E. Yenilmez, Q. Wang, J. P. McVittie, Y. Nishi, J. Gibbons, H. Dai, *Proc. Natl. Acad. Sci. USA* **2005**, *102*, 16141.
[97] S. Talapatra, S. Kar, S. K. Pal, R. Vajtai, L. Ci, P. Victor, M. M. Shaijumon, S. Kaur, O. Nalamasu, P. M. Ajayan, *Nat. Nanotechnol.* **2006**, *1*, 112.
[98] Y. J. Jung, S. Kar, S. Talapatra, C. Soldano, G. Viswanathan, X. Li, Z. Yao, F. S. Ou, A. Avadhanula, R. Vajtai, S. Curran, O. Nalamasu, P. M. Ajayan, *Nano Lett.* **2006**, *6*, 413.
[99] L. Ci, S. M. Manikoth, X. Li, R. Vajtai, P. M. Ajayan, *Adv. Mater.* **2007**, *19*, 3300.
[100] X. Gui, J. Wei, K. Wang, A. Cao, H. Zhu, Y.Jia, Q. Shu, D. Wu, *Adv. Mater.* **2010**, *22*, 617.
[101] X. Gui, A. Cao, J. Wei, H. Li, Y. Jia, Z. Li, L. Fan, K. Wang, H. Zhu, D. Wu, *ACS Nano* **2010**, *4*, 2320.
[102] A. Kis, G. Csanyl, J. P. Saalvetet, T. Lee, E. Couteau, A.J. Kulik, W. Benonj, J. Brugger, L. Forrò, *Nat. Mater.* **2004**, *3*, 153.
[103] W. Ma, L. Liu, Z. Zhang, R. Yang, G. Liu, T. Zhang, X. An, X. Yi, Y. Ren, Z. Niu, J. Li, H. Dong, W. Zhou, P. M. Ajayan, S. Xie, *Nano Lett.* **2009**, *9*, 2855.
[104] T. V. Sreekumar, T. Liu, S. Kumar, L. M. Ericson, R. H. Hauge, R. E. Smalley, *Chem. Mater.* **2003**, *15*, 175.
[105] X. Zhang, T. V. Sreekumar, T. Liu, S. Kumar, *J. Phys. Chem. B* **2004**, *108*, 16435.
[106] S. Wang, Z. Liang, B. Wang, C. Zhang, *Adv. Mater.* **2007**, *19*, 1257.
[107] J. N. Coleman, W. J. Blau, A. B. Dalton, E. Muñoz, S. Collins, B. G. Kim, J. Razal, M. Selvidge, G. Vieiro, R. H. Baughman, *Appl. Phys. Lett.* **2003**, *82*, 1682.
[108] Z. Wang, Z. Liang, B. Wang, C. Zhang, L. Kramer, *Compos. Part A* **2004**, *35*, 1225.
[109] B. Ashrafi, J. Guan, V. Mirjalili, P. Hubert, B. Simard, A. Johnston, *Compos. Part A* **2010**, *41*, 1184.
[110] P. D. Bradford, X. Wang, H. Zhao, J.-P. Maria, Q. Jia, Y. T. Zhu, *Compos. Sci. Technol.* **2010** *70*, 1980.
[111] A. A. Mamedov, N. A. Kotov, M. Prato, D. M. Guldi, J. P. Wicksted, A. Hirsch, *Nat. Mater.* **2002**, *1*, 190.
[112] M. Olek, J. Ostrander, S. Jurga, H. Möhwald, N. Kotov, K. Kempa, M. Giersig, *Nano Lett.* **2004**, *4*, 1889.
[113] Q. Cheng, J. Wang, K. Jiang, Q. Li, S. Fan, *J. Mater. Res.* **2008**, *23*, 2975.
[114] Y. Gao, J. Li, L. Liu, W. Ma, W. Zhou, S. Xie, Z. Zhang, *Adv. Funct. Mater.* **2010**, *20*, 3797.
[115] S. B. Cronin, A. K. Swan, M. S. Ünlü, B. B. Goldberg, M. S. Dresselhaus, M. Tinkham, *Phys. Rev. B* **2005**, *72*, 035425.
[116] S. B. Cronin, A. K. Swan, M. S. Ünlü, B. B. Goldberg, M. S. Dresselhaus, M. Tinkham, *Phys. Rev. Lett.* **2004**, *93*, 167401.
[117] G. Ma, Y. Ren, J. Guo, T. Xiao, F. Li, H. Cheng, Z. Zhou, K. Liao, *Appl. Phys. Lett.* **2008**, *92*, 083105.
[118] M. R. Falvo, G. J. Clary, R. M. Taylor, V. Chi, F. P. Brooks, Jr., S. Washburn, R. Superfine, *Nature* **1997**, *389*, 582.
[119] V. Sazonova, Y. Yaish, H. Üstünel, D. Roundy, T. A. Arias, P. L. McEuen, *Nature* **2004**, *431*, 284.
[120] D. Qian, G. J. Wagner, W. K. Liu, M. F. Yu, R. S Ruoff, *Appl. Mech. Rev.* **2002**, *55*, 495.
[121] A. Cao, P. L. Dickrell, W. G. Sawyer, M. N. Ghasemi-Nejhad, P. M. Ajayan, *Science* **2005**, *310*, 1307.
[122] C. P. Deck, J. Flowers, G. S. B. McKee, K. Vecchio, *J. Appl. Phys.* **2007**, *101*, 023512.
[123] S. B. Hutchens, L. J. Hall, J. R. Greer, *Adv. Funct. Mater.* **2010**, *20*, 2338.
[124] J. Suhr, P. Victor, L. Ci, S. Sreekala, X. Zhang, O. Nalamasu, P. M. Ajayan, *Nat. Nanotechnol.* **2007**, *2*, 417.
[125] J. N. Coleman, U. Khan, W. J. Blau, Y. K. Gun'ko, *Carbon* **2006**, *44*, 1624.
[126] R. J. Mora, J. J. Vilatela, A. H. Windle, *Compos. Sci. Technol.* **2009**, *69*, 1558.
[127] J. Li, L. Hu, L. Wang, Y. Zhou, G. Grüner, T. J. Marks, *Nano Lett.* **2006**, *6*, 2472.
[128] C. M. Aguirre, S. Auvray, S. Pigeon, R. Izquierdo, P. Desjardins, R. Martel, *Appl. Phys. Lett.* **2006**, *88*, 183104.

[129] R. A. Hatton, A. J. Miller, S. R. P. Silva, *J. Mater. Chem.* **2008**, *18*, 1183.
[130] D. Y. Khang, J. Xiao, C. Kocabas, S. MacLaren, T. Banks, H. Jiang, Y. Y. Huang, J. A. Rogers, *Nano Lett.* **2008**, *8*, 124.
[131] Z. Fan, J. C. Ho, T. Takahashi, R. Yerushalmi, K. Takei, A. C. Ford, Y. L. Chueh. A. Javey, *Adv. Mater.* **2009**, *21*, 3730.
[132] Q. Cao, S. H. Hur, Z. T. Zhu, Y. Sun, C. Wang, M. A. Meitl, M. Shim, J. A. Rogers, *Adv. Mater.* **2006**, *18*, 304.
[133] B. Shan, K. J. Cho, *Phys. Rev. Lett.* **2005**, *94*, 236602.
[134] C. Kocabas, H. S. Kim, T. Banks, J. A. Rogers, A. A. Pesetski, J. E. Baumgardner, S. V. Krishnaswamy, H. Zhang, *Proc. Natl. Acad. Sci. USA* **2008**, *105*, 1405.
[135] K. H. An, W. S. Kim, Y. S. Park, J. Mi Moon, D. J. Bae, S. C. Lim, Y. S. Lee, Y. H. Lee, *Adv. Funct. Mater.* **2001**, *11*, 387.
[136] S. Claye, J. E. Fischer, C. B. Huffman, A. G. Rinzler, R. E. Smalley, *J. Electrochem. Soc.* **2000**, *147*, 2845.
[137] S. H. Ng, J. Wang, Z. P. Guo, J. Chen, X. Wang, H. K. Liu, *Electrochim. Acta* **2005**, *51*, 23.
[138] C. Niu, E. K. Sichel, R. Hoch, D. Moy, H. Tennent, *Appl. Phys. Lett.* **1997**, *70*, 1480.
[139] V. L. Pushparaj, M. M. Shaijumon, A. Kumar, S. Murugesan, L. Ci, R. Vajtai, R. J. Linhardt, O. Nalamasu, P. M. Ajayan, *Proc. Natl. Acad. Sci. USA* **2007**,*104*, 13574.
[140] P. C. Chen, G. Shen, S. Sukcharoenchoke, C. Zhou, *Appl. Phys. Lett.* **2009**, *94*, 043113.
[141] A. Izadi-Najafabadi, S. Yasuda, K. Kobashi, T. Yamada, Don N. Futaba, H. Hatori, M. Yumura, S. Iijima, K. Hata, *Adv. Mater.* **2010**, *22*, E235.
[142] A. A. Zakhidov, D. S. Suh, A. A. Kuznetsov, J. N. Barisci, E. Munōz, A. B. Dalton, S. Collins, Von H. Ebron, M. Zhang, J. P. Ferraris, A. A. Zakhidov, R. H. Baughman, *Adv. Funct. Mater.* **2009**, *19*, 2266.
[143] V. P. Veedu, A. Cao, X. Li, K. Ma, C. Soldano, S. Kar, P. M. Ajayan, M. N. Ghasenmi-Nejhad, *Nat. Mater.* **2006**, *5*, 457.
[144] E. J. García, B. L. Wardle, A. J. Hart, *Compos. Part A* **2008**, *39*, 1065.
[145] A. Cao, V. P. Veedu, X. Li, Z. Yao, M. N. Ghasemi-Nejhad, P. M. Ajayan, *Nat. Mater.* **2005**, *4*, 540.
[146] M. Majumder, N. Chopra, R. Andrews, B. J. Hinds, *Nature* **2005**, *438*, 44.
[147] A. Srivastava, O. N. Srivastava, S. Talapatra, R. Vajtai, P. M. Ajayan, *Nat. Mater.* **2004**, *3*, 610.
[148] X. Li, G. Zhu, J. S. Dordick, P. M. Ajayan, *Small* **2007**, *3*, 595.
[149] M. Yu, H. H. Funke, J. L. Falconer, R. D. Noble, *Nano Lett.* **2009**, *9*, 225.

Received: December 6, 2010
Published online: April 20, 2011

